Ecosystems (2018) 21: 1073–1087
https://doi.org/10.1007/s10021-017-0205-1

ECOSYSTEMS

© 2017 Springer Science+Business Media, LLC, part of Springer Nature

No Longer a Paradox: The Interaction Between Physical Transport and Biological Processes Explains the Spatial Distribution of Surface Water Methane Within and Across Lakes

Tonya DelSontro,* Paul A. del Giorgio, and Yves T. Prairie

Groupe de Recherche Interuniversitaire en Limnologie (GRIL), Département des Sciences Biologiques, Université du Québec à Montréal, Succ. Centre-Ville, Case postale 8888, Montréal, Québec H3C 3P8, Canada

ABSTRACT

Lakes play an important role in the global carbon cycle, emitting significant amounts of the carbonic greenhouse gases, CO_2 and methane (CH_4). Nearly all lake studies have reported oxygenated surface waters oversaturated with (and thus continuously emitting) CH_4, yet no consistent explanation exists to account for why CH_4, which is produced in anoxic zones and consumed in the presence of oxygen, remains in oxic waters across the range of lake sizes. Here, we developed a physical model that defines the spatial CH_4 distribution in the surface waters of lakes as a function of CH_4 transport from the littoral zone including air–water gas exchange, and tested this in a set of 14 lakes that ranged widely in size (0.07–19,000 km^2). Although the model adequately resolved the overall CH_4 decline within a lake relative to distance from shore across the range of lake sizes, discrepancies between observations and predictions suggest that other processes modulate surface CH_4 distributions. Coupled trends in the stable carbon isotopic signature of CH_4 further indicate that the spatial pattern in 30% of the lakes was dominated by a net loss via oxidation, whereas a net input of ^{13}C-depleted CH_4 dominated the spatial pattern in 70% of the lakes, suggesting the predominance of pelagic CH_4 production in the oxic epilimnia of these lakes. The spatial patterns imposed by the interaction between physical and biological processes may result in a size-dependent underestimation of whole-lake CH_4 emissions when based on center samples. Whereas the actual contributions of oxidation and eplimnetic CH_4 production are still not well understood, our results demonstrate that the ubiquitous CH_4 oversaturation observed in most

---

Received 4 August 2017; accepted 5 November 2017;
published online 27 November 2017

Electronic supplementary material: The online version of this article (https://doi.org/10.1007/s10021-017-0205-1) contains supplementary material, which is available to authorized users.

Author Contribution All authors identified the research questions, designed the study approach and wrote the manuscript. TD performed the research. YTP and TD derived the model. TD and YTP analyzed and modelled the data.

Data Archiving: Data used for this study can be found in the associated supplemental information and on the Open Science Framework at https://osf.io/wgfvr/?view_only=4be27ba9692848b4a356114bc9a8bd4a.

*Corresponding author; e-mail: tdelsontro@gmail.com

lakes can be explained through the interaction between horizontal transport of littoral CH_4, air–water gas exchange and the balance between epilimnetic CH_4 oxidation and production.

Key words: carbon; inland waters; reservoirs; gas exchange; littoral; horizontal transport; oxic production; oxidation.

INTRODUCTION

It has now been unambiguously established that the vast majority of lakes, particularly in northern temperate and boreal landscapes, act as net sources of CH_4 to the atmosphere (Juutinen and others 2009; Bastviken and others 2011; Rasilo and others 2015; Wik and others 2016; Rinta and others 2017). These lake emissions are significant from a carbon perspective and may partly offset terrestrial carbon uptake globally (Bastviken and others 2011). Most studies to date have focused on the pelagic areas of lakes and have consistently reported CH_4 supersaturation across the whole spectrum of systems, including epilimnetic waters of large and deep lakes during summer stratification (for example, Juutinen and others 2009; Rasilo and others 2015). Persistent system-wide supersaturation requires that the input of CH_4 to open waters exceed the losses of CH_4 through biological oxidation (Reeburgh and Heggie 1977) and air–water gas exchange (Bastviken and others 2004). The fact that epilimnetic waters are generally well-oxygenated and well-mixed, and that vertical CH_4 diffusion from anoxic hypolimnia is generally negligible (Peeters and others 1996), has led to questions concerning the source of epilimnetic CH_4 supersaturation and thus to the notion of the 'methane paradox' (Schmidt and Conrad 1993; Grossart and others 2011; Tang and others 2014, 2016).

This apparent paradox of persistent CH_4 supersaturation in the epilimnion of stratified lakes has in turn led to the hypothesis that the CH_4 in open surface waters must originate from the narrow band of anoxic sediment in contact with the epilimnion along the perimeter of a lake [that is, littoral zone; Figure S1 in Supplemental Information (SI)]. A dominant littoral source of CH_4 would necessarily impose horizontal gradients in CH_4 concentrations from shore to lake center in the epilimnia of stratified lakes, as a portion of CH_4 is continually lost to the atmosphere, and there is indeed evidence of significant spatial variability in lacustrine CH_4 concentrations (for example, Murase and others 2005; Hofmann 2013; Schilder and others 2013). In particular, the observation that littoral concentrations tend to be on average higher than those found in open waters in small- to medium-sized lakes has been interpreted as definitive evidence that the littoral must be the main source of open water supersaturation in lakes in general (for example, Fernández and others 2016). Although this conclusion is consistent with the observed pattern, it is also a major oversimplification of the problem given the complexity of turbulent and advective horizontal transport processes in lakes. More generally, the persistent oversaturation needs to be quantitatively reconciled with the amount of CH_4 generated in the littoral area, the nature and speed of horizontal CH_4 transport from the littoral zone, and the losses of CH_4 due to atmospheric exchange and oxidation during transit.

Whereas it is intuitive that, in small lakes, the lateral transport of CH_4 from the littoral zone may dominate this balance, and thus largely explain the persistence of CH_4 supersaturation in open waters, this scenario cannot necessarily be extrapolated to all lakes, especially larger ones. As lake size and transit distances increase, the importance of losses relative to inputs likely increases, despite the fact that horizontal diffusivity also increases with lake size (for example, Peeters and others 1996). Regardless, there may potentially be a threshold of lake size beyond which the littoral source cannot physically sustain center lake CH_4 supersaturation, given the physical limits of horizontal dispersion and prevailing air–water gas exchange. Moreover, CH_4 oxidation likely further modulates the impact of purely physical constraints by altering the spatial pattern of CH_4 at the whole-lake scale. No study to date, however, has explicitly quantified the balance between transport and loss processes across a range of lake sizes. To complicate matters further, recent reports have suggested that CH_4 may actually be produced in the oxic water column of lakes (Grossart and others 2011; Bogard and others 2014; Yao and others 2016; Wang and others 2017). Such a pelagic source, depending on its spatial heterogeneity, might impose a baseline level of ambient CH_4 that is independent of transport from littoral areas, which would become relatively more important as lake surface area increases and connectivity to littoral sediment sources decreases.

It is clear that in spite of much recent research on freshwater CH_4 dynamics, we are still far from a complete understanding of what drives CH_4 supersaturation in open waters across a range of lake sizes, and this, in turn, hampers our capacity to robustly predict how aquatic CH_4 emissions may shift under scenarios of environmental and climate change. Understanding the mechanisms underlying the large spatial heterogeneity that exists in lake CH_4 concentrations within lakes is key to deriving more effective sampling schemes and thereby more robust estimates of whole-lake CH_4 emissions, a pre-requisite to upscaling fluxes from local to larger scales.

What is needed to address this limitation is the ability to reconstruct the actual shape of the inshore–offshore spatial pattern in lake CH_4 concentration on the basis of realistic combinations of lateral transport and loss and production processes within and across lakes of various sizes. Here we address this fundamental objective by using detailed inshore to offshore transects of CH_4 concentration and stable carbon isotopic composition ($^{13}CH_4$) across 14 lakes that span six orders of magnitude in size. First, we develop a simple physical model that incorporates littoral sources and horizontal transport of CH_4, as well as air–water CH_4 exchange, and apply this model to our study lakes to assess how much of the observed spatial patterns may be explained by physical processes alone. This physical model was then validated against the measured spatial distribution of radon, a radioactive and biologically inert gas that is mainly injected into lakes through littoral groundwater inputs. We complemented the physical model with a coupled spatial mass balance of $^{13}CH_4$ to assess the potential role of biological processes (that is, CH_4 oxidation and epilimnetic CH_4 production) in further modulating the spatial patterns in CH_4, and in particular, to determine how this role may change along a gradient of lake sizes. Finally, we use this coupled physical–biological model to establish the limits of littoral CH_4 delivery to open waters as a function of lake size, and to assess the potential influence of the resulting spatial patterns on our estimates of whole-lake CH_4 emissions.

METHODS

Sampling Strategy

We sampled 14 lakes (12 in Québec, Canada, as well as Lake Ontario (Ontario, Canada) and Lake Champlain (NY, USA); Table S1) in summer 2015. In each lake, we sampled along a transect from the shore (at a spot not located within a bay) toward the center and/or deepest part of the lake and in the direction of the prevailing wind that day. Using bathymetry data, sampling locations along the transect were chosen to adequately cover the depth gradient, with samples in waters overlying where the epilimnion, metalimnion and hypolimnion intersect the sediment. This resulted in 13–18 locations per lake with the highest density close to shore where the depth increases fastest. At each location, samples were taken for dissolved gas using the headspace technique. We filled a 1-l bottle with 500 ml of surface water and 500 ml of ambient air, equilibrated by shaking for 2 min and then used a peristaltic pump to fill the bottle from the bottom with lake water and displace the headspace into a super-inert foil gas sampling bag (Sigma-Aldrich Canada Co., Canada). Replicates were taken at each sampling location. Prior to filling the gastight bag from one of the replicates, we took replicate samples for stable carbon isotopic composition of CH_4 ($\delta^{13}CH_4$) using a 60-ml syringe and injecting gas into 12-ml vials (Labco, UK), slightly over pressurizing for complete filling of the vials. Water samples for radon analysis were collected approximately 50 cm below the surface in 2-l bottles at four to five locations along each lake transect. The bottles were closed air-free under water.

Sample Analysis

Headspace CH_4 concentrations were measured on an ultraportable greenhouse gas analyzer (UGGA, ABB-Los Gatos Research, USA) from the foil sampling bags each evening following sampling. Dissolved CH_4 concentration in lake surface water was calculated according to the headspace ratio, analysis and field temperatures of the water, and the ambient air concentration on the day of sampling also measured via the UGGA. $\delta^{13}CH_4$ was measured in the laboratory using a cavity ring-down spectrometer (CRDS) equipped with a small sample isotopic module (SSIM, Picarro G2201-i, Picarro Inc, CA, USA). Sub-samples for $\delta^{13}CH_4$ were taken from vials collected in the field via gastight glass syringes. For samples with CH_4 concentrations less than 200 μatm, 20 ml of sample was injected directly into the SSIM for analysis. For samples exceeding 200 μatm, samples were also directly injected into the SSIM but diluted using ultra-pure zero air (Praxair Canada Inc., Canada) via the dilution capability of the SSIM to avoid possible interference of laser paths at high CH_4 concentrations. Isotopic data are reported in the standard delta (δ) notation expressed in per mil (‰) relative to the standard Vienna Pee Dee Belemnite (Whiticar 1999). The calibration of $\delta^{13}CH_4$ values were performed using three certified isotopic standards (Liso1, − 66.5 ± 0.2‰; Tiso1, − 38.3 ± 0.2‰; Hiso1, − 23.9 ± 0.2‰; Isometric Instruments, Canada). Final $\delta^{13}CH_4$ values were corrected for isotopic mixing with ambient air using the mean of all $\delta^{13}CH_4$ values for 44 air samples (− 50.04 ± 1.07‰) taken over the course of the campaign. A Monte Carlo simulation of 1000 iterations was run on each final isotopic value to determine an error threshold for headspace CH_4 concentrations that approached ambient air CH_4 concentrations, and when the threshold was crossed that sample was disregarded due to low confidence in its isotopic signature. Ultimately, we disregarded all L. St-Jean samples from isotopic analyses, as well as five from Lake Ontario, four from Lake Simard, three from Lake Achigan, and two from Lake Nominingue. ^{222}Rn activity (in units, Bq m^{-3}) was measured using a portable radon detector (RAD7, Durridge Company Inc., USA) from a 30-ml headspace connected via a closed-loop system (RadH$_2$O) to the water sample. An air stone was deployed in the water sample for ~ 2 h to induce equilibrium of radon between the sample and the headspace prior to measurement. ^{222}Rn measurements were corrected for temperature and humidity, which were simultaneously measured during analysis, as well as for fractionation and decay. As radon activity is a result of groundwater inflows, which we did not have prior knowledge of in each lake, measureable radon was only found in some lakes.

Conceptual Model Framework

Dissolved CH_4 found in the center of a lake has three potential sources: (1) diffusion from sediments and the water column below (Bastviken and others 2004), (2) dissolving bubbles emanating from sediments below (McGinnis and others 2006; Varadharajan and Hemond 2012) and (3) horizontal transport from the littoral zone where both diffusion and ebullition from sediments supply CH_4 to shallow waters (Murase and others 2003; Hofmann and others 2010; Schubert and others 2010). Because vertical diffusivity is typically orders of magnitude slower than horizontal diffusivity during the stratified period (Peeters and others 1996), which was when each lake was sampled (Table S1), and because oxidation also regulates vertical CH_4 transfer, we assume that hypolimnetic CH_4 was a negligible source to surface waters. We also assume that dissolution from rising CH_4 bubbles (that is, ebullition) from the deeper parts of lakes was not a source of surface CH_4 as bubbles are not commonly observed from depths deeper than 3 m in Québec lakes (DelSontro and others 2016), similar to boreal lakes of other regions (Bastviken and others 2004). In addition, we surveyed twelve small lakes in 2014 with an echosounder (see Ostrovsky and others 2008; DelSontro and others 2015 for echosounder method details), including four of the lakes in the current study (Table S2). We found no ebullition in depths greater than 2 m from lakes of a size (0.02–0.9 km^2) and maximum depth range (4–23 m) in which ebullition could potentially be a dominant CH_4 source due to dissolution of rising bubbles (for example, an average bubble released from 20 m depth would release 20% of its CH_4 content to the atmosphere; DelSontro and others 2015). Ultimately, by eliminating vertical transfer and ebullition as potential CH_4 sources in our study lakes, we were able to examine if horizontal transport from the littoral zone could account for the CH_4 observed in the center of these non-bubbling, stratified lakes.

Conceptually, our work explicitly examines the null hypothesis that the only source of surface water CH_4 in seasonally stratified lakes is confined to the littoral area where surface waters are in contact with sediments. Two general predictions can be derived from this single hypothesis: one pertaining to among lake variation in CH_4 concentration, while the other applies to within lake heterogeneity. First, if CH_4 production from littoral sediments is assumed to be roughly similar across lakes, we would expect a strong allometric decline in the average CH_4 as a function of lake size simply from geometric scaling arguments since the perimeter-to-area ratio naturally decreases with increasing surface area. This prediction can be easily tested by comparing the average of a representative sample of CH_4 concentrations in lakes of different sizes, and more rigorous prediction can be derived depending on the assumed shape and bathymetry. Second, at the scale of individual ecosystems, the same null hypothesis predicts that CH_4 concentrations should decrease from shore to center in all lakes, although the exact shape of the radial decline is itself expected to vary with lake size. Under steady-state conditions, the concentration of CH_4 at any point x (C_x, expressed as excess concentration relative to atmospheric equilibrium) along a transect from shore to center is, from physical forces alone, the net result of the rates of horizontal dispersion of the gas (represented by the effective horizontal diffusivity coefficient, k_H

[$m^2\ d^{-1}$]) relative to evasion of the gas to the atmosphere (represented by the standardized gas exchange coefficient, k_{600} [$m\ d^{-1}$]) from the upper mixed layer of the lake (Z_{ML} [m]). k_H describes the dispersion of dissolved substances in a water body that results from both turbulent diffusion related to eddy diffusivity and large-scale flow (Peeters and Hofmann 2015). The governing differential equation for this process is thus given by

$$k_H \frac{\partial^2 C(x)}{\partial x^2} = \frac{k_{600}}{Z_{ML}} C_x. \qquad (1)$$

The exact solution of equation 1 will depend on an assumed lake shape configuration and on boundary conditions. In this work, we have considered two configurations representing extremes of lake shape: perfectly round and infinitely elongated lakes where transport from the far edges is negligible. For the round configuration, we imposed boundary conditions that the edge concentration is uniform around the lake and that there is no net flow of CH_4 in any radial direction at the lake center, while for the elongated configuration, we relaxed the assumption and allowed the two opposing shores to have different initial conditions, yielding, respectively, the following solutions:

$$C_x = C_C I_0(\lambda(r_L - x)) \quad \text{(round)} \qquad (2)$$

and

$$C_x = C_{0(n)} e^{-\lambda \cdot x} + C_{0(f)} e^{-\lambda \cdot (D-x)} \quad \text{(elongated).} \qquad (3)$$

In equation 2, I_0 is the modified Bessel function of the first kind of order 0, r_L is the radius (m) of the lake, x is distance (m) from shore, and C_C is the CH_4 concentration at the lake's center. In the elongated configuration (equation 3), D (in m) is the distance between the two shores of the short axis and $C_{0(n)}$ and $C_{0(f)}$ are constants that can be loosely interpreted as the near and far shore concentrations, respectively. See SI for details on the derivations of these solutions.

In both models and for simplicity, we define

$$\lambda = \sqrt{\frac{k_{600}/Z_{ML}}{k_H}} \qquad (4)$$

which is a compound metric (in units of m^{-1}) describing the decline in concentration from shore to center due to physics alone. However, all three components of λ (k_{600}, k_H, Z_{ML}) are known to scale positively but differently with lake size (for example, Hanna 1990; Vachon and Prairie 2013; Peeters and Hofmann 2015) and, as a result, it is difficult to infer the overall relationship between λ and lake size. As a first step, we examined this question using empirical models from the literature. We used the lake area, A [km^2], and wind at 10 m, U_{10} [$m\ s^{-1}$], model from Vachon and Prairie (2013) to predict average k_{600}:

$$k_{600} = 2.51 + 1.48U_{10} + 0.39U_{10}\log_{10}(A). \qquad (5)$$

U_{10} was calculated from surface wind speed measured at each sampling location via Crusius and Wanninkhof (2003):

$$U_{10} = U_z * \left(1 + \frac{(C_d)^{0.5}}{K} \ln\left(\frac{10}{z}\right)\right) \qquad (6)$$

where U_z is the measured wind speed at height z (1.5 m in our case), C_d is the drag coefficient at 10 m (0.0013 from Stauffer 1980) and K is the von Karman constant (0.41). We found a linear relationship (overall $r^2 = 0.64, p < 0.0001, n = 235$) between the $\log_{10}$-transformations of distance from shore (that is, fetch) and U_{10} calculated from all wind speeds measured 1.5 m above the lake surface. The U_{10}-fetch relationship maintained the same slope (0.211) in each lake but with a different intercept (Table S3). We used the slope and lake-specific intercept to find U_{10} for each sampling location within a lake and used the average of those U_{10} values in equation 5 to provide an integrated k_{600} for the lake.

To estimate k_H, we used two literature models (Lawrence and others 1995; Peeters and Hofmann 2015) (Table S3):

$$k_{H1} = 1.4 \times 10^{-4} L^{1.07} \quad \text{(Peeters and Hofmann 2015)} \qquad (7)$$

$$k_{H2} = 3.2 \times 10^{-4} L^{1.10} \quad \text{(Lawrence and others 1995)} \qquad (8)$$

where L [m] is length scale. Because we were interested in whole-lake scale dispersion, L was calculated as $L = \sqrt{2\sigma_{ma}\sigma_{mi}}$ where σ_{ma} and σ_{mi} are the standard deviations of the major and minor axes of the lake contour vertices, respectively (Table S3; Okubo 1971; Peeters and others 1996). The two horizontal diffusivity k_H models differ by a factor of about 3, regardless of length scale, and provide reasonable upper and lower bounds of horizontal dispersion by which to evaluate our model. Equation 7 is the average result from experiments 1, 3 and 4 found in Table 2 of Peeters and Hofmann (2015) and further details regarding k_H are found in the SI. Finally, mixed layer depth, Z_{ML}, can be determined easily in a single sampling visit, and for predictions of Z_{ML} in theoretical lakes we used the relationship found between area and Z_{ML} in our 14 study lakes (Z_{ML} [m] = 3.61 + 1.66 * $\log_{10}$ (Area [km^2]), $r^2 = 0.75$, $p < 0.0001$).

The littoral source model thus far describes the physical transport of littoral CH_4 toward the center of a lake without regard for any possible biologically based modulation of surface CH_4, namely by oxidation or epilimnetic CH_4 production. There are various ways to incorporate these biological processes within our physical model framework. In terms of concentrations, the simplest formulation is to model oxidation as a first-order loss reaction (k_{oxi}, d^{-1}) and epilimnetic production as a constant additional influx of CH_4 (P, mmol m^{-3} d^{-1}) homogeneously distributed over the entire lake. Solution of our models (equations 2 and 3 for round and elongated) with these processes would simply modify the λ parameter to

$$\lambda = \sqrt{\frac{k_{600}/Z_{ML} + k_{oxi}}{k_H}} \quad (9)$$

and include an additive term $[CH_4]_P$ representing the concentration of CH_4 sustained by the pelagic production under given oxidation and gas evasion conditions equal to

$$[CH_4]_P = \frac{P}{k_{600}/Z_{ML} + k_{oxi}}. \quad (10)$$

However, simulations using realistic values for k_{oxi} and P (Table S4) suggest that although these processes can alter the absolute CH_4 concentrations substantially, the expected changes in the shape of the horizontal profiles induced by the biological reactions are modest and unlikely to be distinguishable from other sources of uncertainty.

Quantifying the Net Impact of Biological Processing on Surface CH_4 Using Stable Isotopes

To further resolve the relative importance of the two biological processes, we integrated our physical framework with a stable isotope fractionation model in a simplified conceptualization of the oxidation/production processes. Instead of treating them separately as in equations 9 and 10, we considered them as opposite reactions that can be integrated readily into our physical modeling framework as a single additive (positive for oxidation and negative for production) term $k_{O/P}$ [d^{-1}] in (λ):

$$\lambda = \sqrt{\frac{k_{600}/Z_{ML} + k_{O/P}}{k_H}} \quad (11)$$

Here, this new term $k_{O/P}$ should be viewed as an integrative measure of the net impact of biological processes (oxidation and pelagic production) on surface CH_4, expressed as a specific rate coefficient (in d^{-1}). The critical advantage of this simpler formulation is that, when combined with an open-system isotopic model (Happell and Chanton 1994; see SI for details), it allows direct derivation of a first-order estimate of $k_{O/P}$ for each lake from the relationship linking the $\delta^{13}CH_4$ signature of samples in lake i to the corresponding concentrations, $[CH_4]$, of those samples:

$$\ln\left(((\alpha - 1) \times 1000) - (\delta^{13}CH_{4_i} - \delta_s)\right) = \beta_0 + \beta_1 \ln([CH_4]_i) \quad (12)$$

where $\alpha = 1.02$ is the fractionation factor derived in Bastviken and others (2002), δ_s is the $\delta^{13}C$ of the source CH_4, which would be littoral-derived CH_4 and can be approximated by the intercept of a Keeling plot (that is, $1/[CH_4]$ versus $\delta^{13}CH_4$; Keeling 1958). β_0 is the intercept of the relationship produced by relating $[CH_4]$ and $\delta^{13}CH_4$ for each lake and β_1 is the slope of that relationship. The $k_{O/P}$ can then be estimated from linear regression on equation 12 as

$$k_{O/P} = \frac{\beta_1 * k_{600}/Z_{ML}}{(1 - \beta_1)}. \quad (13)$$

Details on the derivation and assumptions of this model can be found in the SI.

RESULTS AND DISCUSSION

Predictions from Physical Processes Alone

We combined literature models for k_{600} and k_H with our measured Z_{ML} values to make theoretical predictions as to the expected decline in CH_4 and how it changes with lake size. Figure 1 shows the predicted lake CH_4 distributions based on the elongated (dashed lines, blue shading) and round (solid lines, red shading) lake models for a transect from the shore to the center of two lakes, one small (1 km^2) and the other two orders of magnitude larger (100 km^2). True concentrations observed from two round lakes are shown in each panel of Figure 1 (green dots) for comparison. Assuming the same constant input from either shore in the elongated model (that is, $C_{0(n)} = C_{0(f)}$) and from the entire littoral zone in the round model, we find that the expected concentration in the center of a small lake will be between 6 and 24% of the concentration found at the shore in the elongated lake, and between 13 and 41% in the round lake. The importance of the k_H value also becomes obvious

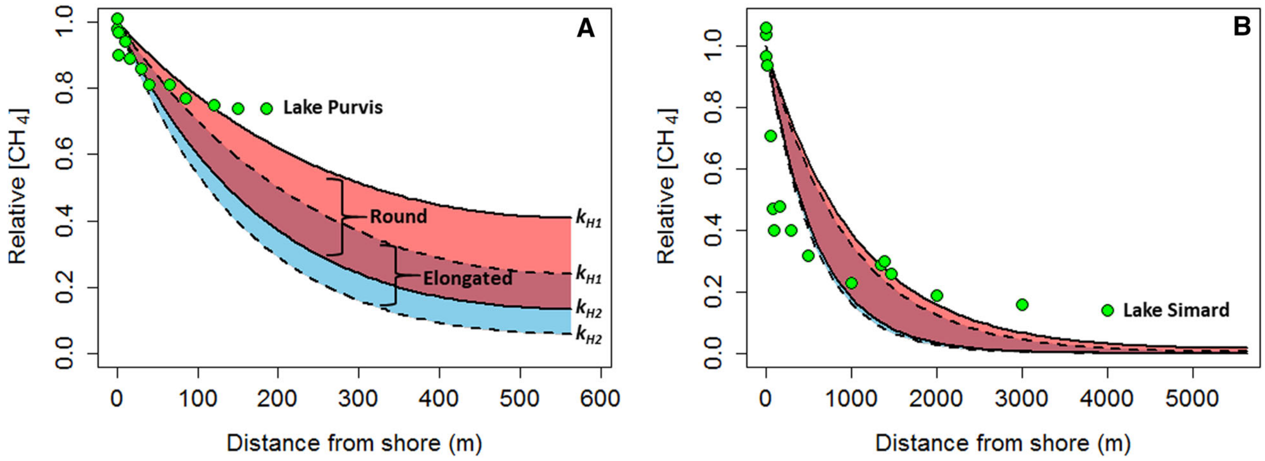

Figure 1. Model predictions of CH_4 distribution in lake surface waters. **A** In a small (1 km^2) lake, the round model (*red shaded area, solid lines*) predicts on average more CH_4 reaching the center of a lake than the elongated model (*blue shaded area, dashed lines*). Upper and lower bounds of each model are based on the different k_H models with the k_{H1} (Peeters and Hofmann 2015) model resulting in more CH_4 reaching the center of the lake than the k_{H2} (Lawrence and others 1995) model. Actual data from Lake Purvis (a slightly smaller, round lake) is shown for comparison (*green circles*). **B** In a large (100 km^2) lake, all physical models predict 1.5% or less of the original CH_4 in the center of the lake. Individual model trends are similar to panel (**A**). Actual data from Lake Simard (a round lake) is shown in which CH_4 was indeed observed in the center of the lake (*green circles*) (Color figure online).

when comparing CH_4 concentrations as a function of distance in the two lake sizes. Although up to 41% of CH_4 remains at 570 m from shore in the example small lake, up to 60% of CH_4 remains at the same distance in the example large lake. This is because k_H increases with lake size much faster than either k_{600} or Z_{ML}, and although this ultimately means that λ will decline strongly with lake area, the higher k_H of a large lake will also transport CH_4 faster and further than the lower k_H in a small lake. Not surprisingly, the round lake model results in higher center CH_4 concentrations than the elongated one because it accounts for inputs from all radial directions. However, this difference is only apparent in small lakes as the two models result in similar predictions for larger lakes (Figure 1B). In particular, both the elongated and round models predict negligible CH_4 concentrations at the center of large lakes (> 100 km^2) relative to shore concentrations (for example, $< 1.5\%$ at ~ 5700 m from shore in Figure 1B).

Physical Drivers Dictate Surface CH_4 Concentrations Across and Within Lakes

Before evaluating whether our physical transport model and hypothesis based on a littoral source were supported by our study results, we confirmed that indeed the sampled surface waters of our 14 lakes that spanned six orders of magnitude in size were consistently oversaturated in CH_4 (Figure S2; Table S5). In addition, both the observed concentrations and their spatial distributions were in agreement with the two main predictions stemming from our initial hypothesis that the littoral area is the principal source of surface water CH_4. First, the average surface CH_4 concentrations of our lakes declined with increasing lake area as expected ($R^2 = 0.68$, $p = 0.0003$; Figure S3). These findings imply that ecosystem size is a critically important variable to consider when upscaling aquatic CH_4 emissions regionally or even globally, and that the dispersion and subsequent dilution of CH_4 generated in littoral areas is likely the main driver of this relationship. Further, the strength of the relationship also suggests that the rate of CH_4 input from this littoral source varies little among lakes.

Second, CH_4 concentrations in all but two lakes showed a significantly decreasing trend with distance from shore (Figure 1 and Figures S4 and S5) that strongly mimics the spatial patterns generated by our models based on physical processes alone. To quantitatively compare our field observations with the predictions from the model, we statistically fitted our CH_4 data for each lake using a nonlinear algorithm to either the round or elongated lake physical models (equations 2 and 3) and estimated an empirical λ for each lake. We classified lakes as round or elongated based on their aspect ratio, which was defined as σ_{ma}:σ_{mi}. Since sampling was typically conducted along the shorter lake axis (σ_{mi}), we used the round model for lakes that had an aspect ratio below 3, and elongated for those above 3. Ultimately, 11 lakes were considered round and the remaining three lakes were considered elongated (Tables S1 and S6). Next, we compared the empirical (fitted) λ to a theoretical λ calculated for each lake using the literature models for k_{600} and k_{H}, and assessed how they both varied with ecosystem size (Figure 2, black circles). First, we found a strong relationship between the observed and theoretical λs across our dataset ($r^2 = 0.87$, $p < 0.0001$), demonstrating that the physical transport models largely accounted for the spatial trends in lake surface CH_4. In addition, the observed λ, the metric of the rate of radial decline in CH_4 within a lake, was negatively correlated with lake area, similar to the average CH_4-lake area relationship reported above (Figure S3), which further supports the littoral dispersion hypothesis. As a further validation of the role of physical processes in driving the spatial pattern in gas concentrations, we performed the same analysis using radon (after correcting for radioactive decay) for the subset of lakes where we had carried out parallel measurements of radon concentration (details in SI). We found that the decline from shore to center estimated from the radon horizontal profiles also followed the same trend with lake area (Figure 2, red triangles; Table S6).

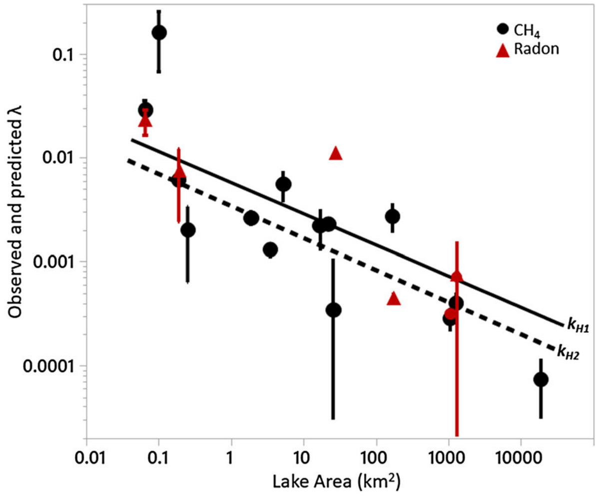

Figure 2. Observed and predicted λ as a function of lake area. Observed λ is the slope of the observed CH_4 concentrations with distance from shore (*black circles*), while the predicted λ are shown as the linear trend found between lake area and λ calculated with average k_{600}, true Z_{ML}, and either k_{H1} (*black line*; Peeters and Hofmann (2015)) or k_{H2} [*dashed line*; Lawrence and others (1995)]. Observed λ for radon are shown for six lakes in which sufficient data were collected (*red triangles*). Error bars are standard error of fitted data (Color figure online).

The Modulating Role of Biological Processes

Despite the strong evidence that physical processes are largely responsible for the observed differences in spatial surface CH_4 concentration both among and within lakes (Figure 2), our models nevertheless failed to reproduce key elements of our field observations. First, the observed λ for many of the lakes was lower than expected from the models based on gas evasion and horizontal dispersion (Figure 2; Table S6), which implies that the physical models systematically under-predicted actual CH_4 concentrations. In addition, while most individual lake CH_4 transects displayed the expected exponential (or Besselian) decrease with distance from shore, two did not show any clear horizontal patterns (L. Achigan and L. Morency, Figures S4 and S5). Similarly, our data contradict the model prediction that CH_4 should be close to or at atmospheric equilibrium at the center of large lakes since we observed CH_4 concentrations consistently in excess of atmospheric equilibrium (which is approximately 0.003 µM) in the center of our largest sampled lakes (Champlain, St-Jean, and Ontario; Table S5, Figure S2). Similar results have been observed in other surveys of central lake CH_4 concentrations, for example, in 224 lakes across Québec (Rasilo and others 2015) and 207 lakes across Finland (Juutinen and others 2009). Both surveys found a large range in CH_4 concentrations that were consistently above saturation, even in lakes up to and over 100 km². Furthermore, in two of our study lakes similar in size to the two example lakes of Figure 1, we see that the equivalent of approximately 80% of the littoral CH_4 remains in the center of the smaller lake (L. Purvis, green points in Figure 1A), whereas about 15% remains in the center of the larger lake (L. Simard, green points in Figure 1B). Not only was atmospheric equilibrium or under saturation not observed in any of our lakes, but central lake CH_4 concentrations remained, on average, 62% of the observed littoral concentrations (Table S5). Lakes close to atmospheric equilibrium with the atmosphere are exceedingly difficult to find in the literature, despite the fact that the majority of reported large-scale CH_4 surveys (for example, Rasilo and others 2015 and Juutinen and others 2009) only sampled lake centers where minimum concentrations are most likely to occur.

It is interesting to explore the limits of physical transport within these lakes in explaining center concentrations of CH_4. Using the k_{H1} and k_{H2} models, our U_{10}-distance model to determine k_{600}, and the lake area-Z_{ML} relationship based on our own data to calculate Z_{ML}, we estimated λ for a series of lakes between 0.01 and 1000 km^2 in area to find the lake size threshold in which our physical transport models could no longer account for dissolved CH_4 found in the center of lakes. We found that using k_{H1} resulted in $< 1\%$ of the littoral CH_4 remaining in the center of lakes larger than 7 and 40 km^2 in size according to the elongated and round models, respectively, whereas k_{H2} allowed lakes to be an order of magnitude larger before central CH_4 concentrations were less than 1% than that of the littoral (90 and 300 km^2 for elongated and round, respectively).

To sum up, although our physical transport model quite adequately captured the overall shape of the spatial distribution of lake surface CH_4, the predictive limitations illustrated above with regard to CH_4 suggest that other important factors are at play. One non-physical process that may strongly modulate surface water concentrations is CH_4 oxidation, which occurs in oxic waters and represents an effective CH_4 sink (for example, Bastviken and others 2002). If oxidation was significant in surface waters of our study lakes, it would result in a steeper decline from shore to center relative to that predicted based on physical processes alone. Only one lake had an observed λ that was substantially higher than the bounds of the modeled λ (Figure 2), whereas the bulk of the lakes had observed λ that were similar or lower than λ predicted from physical processes alone. Therefore, our observations would suggest that CH_4 oxidation likely plays a minor role in determining the spatial patterns in CH_4 concentrations, and instead point to an additional CH_4 source not accounted for in the physical model. This observation is consistent with the hypothesis of pelagic CH_4 production occurring in oxic water columns, which has recently been observed and discussed in other marine (Karl and others 2008; Damm and others 2010) and freshwater systems (Grossart and others 2011; Tang and others 2016; Yao and others 2016; Wang and others 2017), including one of the lakes sampled in our study (Bogard and others 2014).

Although the net impact of biological processing can readily be included in our model structure (that is, as $k_{O/P}$ in equation 11), simulations with realistic rates of $k_{O/P}$ indicating prevalence of either epilimnetic CH_4 production or oxidation suggest that the change in the shape of the spatial CH_4 distribution (Figure 3A; see details in SI and Table S4) would not be distinguishable from the effects of changes in the physical parameterization. Given the natural variability in the physical parameters for lakes of any size (for example, the threefold variability in k_H, Figure 1), we conclude that the relative importance of physical and biological processes cannot be accurately assessed solely on CH_4 concentration trends alone. However, their contribution to surface water CH_4 can be ascertained more directly by examining the contrasting expectations on how the CH_4 isotopic signature, specifically $\delta^{13}CH_4$, should vary in space in response to biological processing.

Isotopic Evidence of Biological Processes Influencing CH_4 Spatial Distribution

In the absence of either biological process, $\delta^{13}CH_4$ is not expected to vary significantly in space because fractionation associated with gas exchange with the atmosphere is minimal (Knox and others 1992), regardless of the patterns in concentrations described earlier (Figure 3A). During CH_4 oxidation, however, the lighter carbon isotope (^{12}C) is preferred and the remaining CH_4 pool becomes ^{13}C-enriched, thereby enabling the use of the resulting $\delta^{13}CH_4$ in a steady-state fractionation model to infer the potential extent of oxidation. Because the net transport of CH_4 via horizontal dispersion proceeds from the shore to the center of a lake, we would expect to detect an oxidation signal as an enriched $\delta^{13}C$ signature of the CH_4 pool along the same radial direction of transport. Conversely, the addition of CH_4 to the transported pool via production in the epilimnion would have the opposite effect on the $\delta^{13}C$ signature of the overall CH_4 pool because this pelagic CH_4 is likely to have a more depleted $\delta^{13}C$ signature than the CH_4 released from littoral sediments, which has already undergone oxidation at the sediment–water interface and during transport. We found via Keeling plots of our individual study lakes that the average $\delta^{13}CH_4$ for littoral CH_4 was $-53.9 \pm 5.4‰$ (Table S7), whereas current evidence suggests that epilimentic CH_4 is produced via acetate fermentation (Bogard and others 2014; Tang and others 2014) and should thus have a $\delta^{13}CH_4$ signature between -50 and $-65‰$ (Whiticar and Faber 1986). Ultimately, the changing proportions of CH_4 originating from dispersion and from epilimnetic production along the horizontal gradient would impact the overall $\delta^{13}CH_4$ signature, thereby allowing us to use the spatial distribution of $\delta^{13}CH_4$ to determine the relative importance of biological processing in modulating overall surface CH_4 distribution.

From a conceptual perspective, we would expect to see one of the three following trends in $\delta^{13}CH_4$ with distance from shore, depending on the pre-

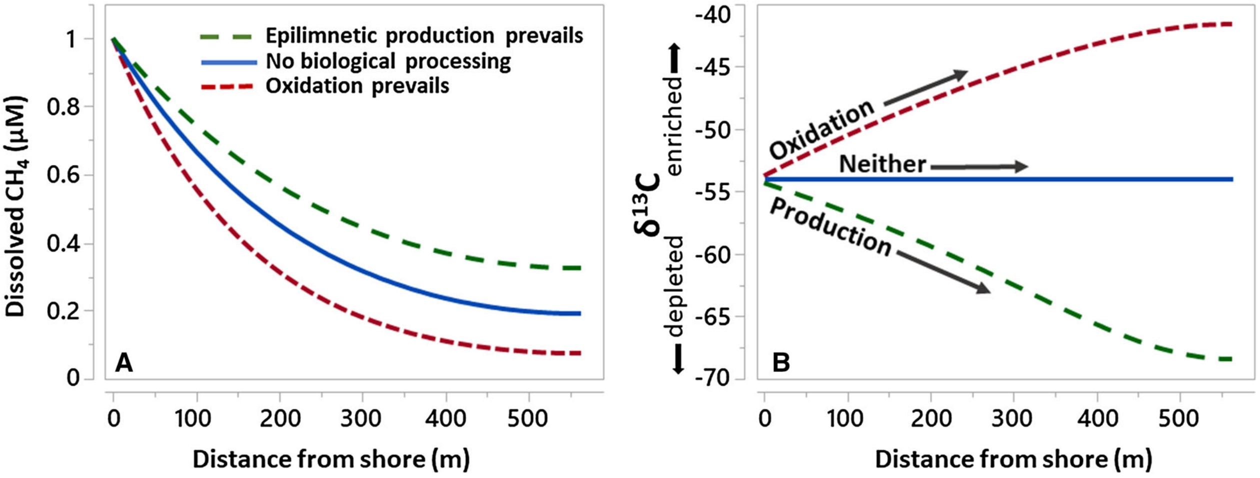

Figure 3. Modulation of surface CH_4 distribution by biological processes. **A** Incorporating either net CH_4 oxidation (here, $k_{O/P}$ = 0.5 d^{-1}) or net epilimnetic CH_4 production (here, $k_{O/P}$ = − 0.18 d^{-1}) into the transport model results in the same dissolved CH_4 trend as that of a physical only transport model, either enhanced or depressed depending in the prevailing process, but ultimately within the uncertainty of the physical model (Figure 1). **B** The δ^{13}C of CH_4, on the other hand, will indicate which biological process dominates during CH_4 transport from shore because they have opposite impacts on the resulting $\delta^{13}CH_4$ trend. A positive slope indicates the CH_4 pool is becoming more enriched (less negative) and thus being oxidized, while a negative slope indicates that the CH_4 pool is becoming depleted (more negative). Depletion can only occur by the mixing of the transported CH_4 pool with CH_4 of a more depleted δ^{13}C signature like that which could come from epilimnetic CH_4 production.

vailing process (Figure 3B): (1) a flat line indicating no change in $\delta^{13}CH_4$, which would suggest either no significant influence of oxidation or production along the transect, or that these processes perfectly balance each other out; (2) a positive slope indicating an increasingly enriched (that is, less negative) $\delta^{13}CH_4$ signature along the transect, suggesting significant oxidation overlying the physical processes; or (3) a negative slope indicating a depleting (that is, more negative) $\delta^{13}CH_4$ signature along the transect, which would suggest a net addition of more δ^{13}C-depleted CH_4 to the transported littoral CH_4 pool. It is important to note that because the oxidation of the transported CH_4 pool can only exhibit a δ^{13}C-enriched signature, the detection of a depleting δ^{13}C signature must indicate the addition of depleted CH_4 to the pool, which is exactly what we found in nine of our study lakes (Figures S4 and S5). Five of these lakes exhibited a $\delta^{13}CH_4$ range of only a few per mil, but four of them had depleting trends ranging from 15 to 30‰. Although the δ^{13}C trends in surface CH_4 indeed indicate that CH_4 is being produced in the oxic epilimnia of 70% of our lakes, oxidation is likely occurring simultaneously. Although from our data, we are unable to calculate an absolute rate for each process, we can nevertheless derive a first-order estimate of the net impact of both processes (that is, $k_{O/P}$, equation 13) based on the surface CH_4 data collected, assuming that production can be roughly modeled as the opposite reaction of oxidation.

Quantifying the Net Impact of Biological Processing on Surface CH_4

Combining our physical transport model with an open steady-state isotopic model revealed that there was significant input from a non-littoral source of CH_4 in the oxic epilimnia of the majority of our lakes, although a few had $k_{O/P}$ values close to a neutral balance such that the prevailing biological process is uncertain (Figure 4). Because $k_{O/P}$ represents the net balance between CH_4 oxidation and eplimnetic CH_4 production, it is not completely appropriate to make a direct comparison with published estimates of either process. Nevertheless, we provide a new compilation of published estimates of CH_4 oxidation and epilimnetic CH_4 production rates (Table S4) to show that the range of our $k_{O/P}$ values (− 0.173 d^{-1} for production to + 0.21 d^{-1} for oxidation; Table S8) all fall within the compiled range (− 1.15 d^{-1} for production to + 3.5 d^{-1} for oxidation).

The shape of the distance-decay function for the coupled CH_4 concentration and $\delta^{13}CH_4$ signature thus integrates and reveals the various processes that influence surface CH_4 spatial dynamics. Ultimately, however, it is the contribution of epilim-

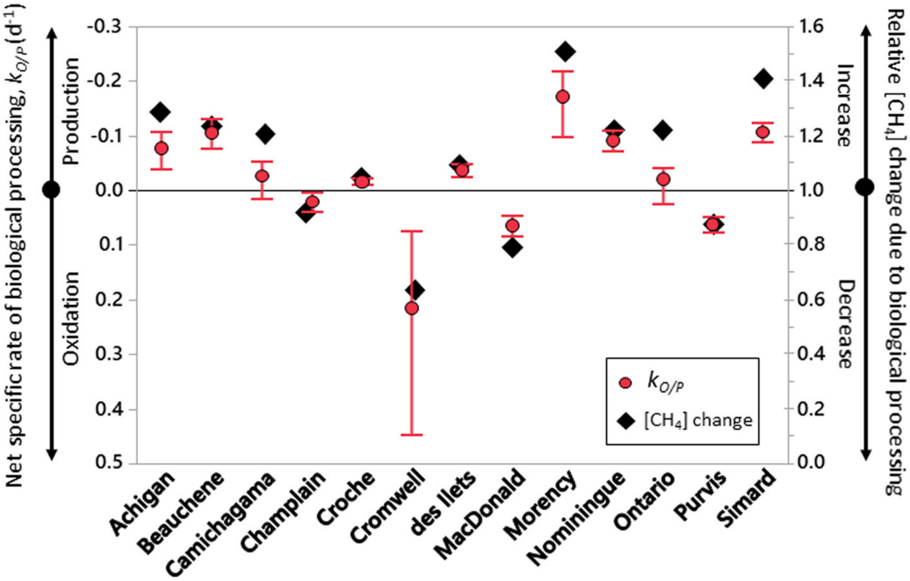

Figure 4. Impact of biological processing on surface CH_4 distribution. *Left axis, red circles*: Net specific rate of the balance between CH_4 oxidation and epilimnetic CH_4 production ($k_{O/P}$, d^{-1}) in lake surface waters. Positive rate indicates oxidation is the prevailing process modulating surface CH_4, whereas a negative rate indicates net epilimnetic CH_4 production. Note the axis is reversed. Error bars are based on standard error of β_1 used to calculate $k_{O/P}$ (equation 13). *Right axis, black diamonds*: Relative increase or decrease in surface CH_4 concentration ([CH_4]) of each lake due to the net rate of the $k_{O/P}$-indicated prevailing process—epilimnetic CH_4 production or oxidation, respectively (Color figure online).

netic biological processes to the "methane paradox," over and above the clear influence of physical processes demonstrated above, that we would need to quantify. To this end, we derived an estimate of the amount by which CH_4 concentrations and emissions were reduced or increased by epilimnetic biological processes by combining $k_{O/P}$ with the average gas residence time, τ_g, within the epilimnion (defined as $\tau_g = Z_{ML}/k_{600}$, in days; Table S8). Systems in which biological processes are fast relative to gas residence time in the mixed layer will exhibit the strongest deviations from physically based expectations. Expressed as a fractional increase or decrease in concentration due to biological processes and estimated as $e^{\tau_g \cdot k_{O/P}}$, our isotope model results suggest that the net impact of biological processes was not trivial, with an average 20% decrease in lakes dominated by oxidation and an average 25% increase in those dominated by a non-littoral CH_4 input (Figure 4, Table S8). It is unlikely that this input was associated to vertical transport of CH_4 from the hypolimnion since at the time of sampling all of these lakes were strongly stratified and molecular diffusion across the thermocline could never account for this flux (Peeters and others 1996). The dissolution of CH_4 bubbles originating from sediments can also be excluded as a potential new source in the epilimnion, since previous studies have shown that CH_4 ebullition is hardly measurable in lake depths beyond 3 to 5 meters, particularly in northern lakes (Bastviken and others 2004; DelSontro and others 2016; Natchimuthu and others 2016). Collectively, these results suggest widespread occurrence of CH_4 production within oxic epilimnia of northern lakes, which in many lakes appear to exceed in magnitude the CH_4 oxidation that occurs in parallel. In a handful of lakes, oxidation quantitatively dominated even if pelagic production might have co-occurred.

The net balance between oxidation and pelagic production strongly modulates the shape of the physically driven distance-decay function and also determines a baseline CH_4 concentration in lake surface water that is largely independent of lateral transport from littoral areas. This balance does not seem to follow a gradient of lake size or trophic status, although oxidation did seem to dominate at higher average CH_4 concentrations. Regardless, it is clear that there is still much to be learnt regarding the mechanisms underlying the inferred shifts in the relative contribution of CH_4 oxidation versus epilimnetic CH_4 production to ambient CH_4 dynamics and concentrations in these northern lakes. For example, in lakes where the two processes are occurring at relatively high rates, we suggest that the prevailing biological process may actually shift along the nearshore to center transect, leading to strong nonlinearity (in equation 12) inconsistent with our modeling approach.

Implications for CH_4 Sampling and Upscaling of System-Wide Emissions

From a more practical perspective, the shape of this distance-decay function has implications for our capacity to accurately quantify CH_4 concentrations in lakes. Previous studies had firmly demonstrated the existence of a relatively large degree of spatial heterogeneity in lake CH_4 concentrations across lakes (Juutinen and others 2009; Rasilo and others 2015), whereas some have also confirmed variability in surface CH_4 within lakes, which undoubtedly adds uncertainty to whole-lake emission estimates (Hofmann 2013; Schilder and others 2013, 2016). The results that we present here further suggest that point measurements taken in the lake center will tend to systematically underestimate integrated, whole-lake CH_4 concentration. Perhaps even more importantly, our results also suggest that the magnitude of this bias is not constant, but rather varies as a function of two parameters: (1) lake size, because of its influence on the distance-decay curve (Figure 2), and (2) the strongly modulating influence of epilimnetic biological processes. By integrating our model solutions (equations 2 and 3) over the entire surface of the two model shapes (round and elongated; see SI for derivation), we can derive formulas for the expected ratio of the center CH_4 concentration to the spatially integrated CH_4 concentration for a lake, hereafter called the underestimation ratio. A value close to unity would imply that the center concentration is similar to the integrated concentration (that is, little to no underestimation), while lower values imply that a correction would need to be applied to obtain an unbiased estimate of lake-wide concentrations (and thereby emissions) from samples obtained from the center of lakes. We examined the magnitude of this underestimation bias as a function of lake size under various scenarios. Using only the physical components of the model (Z_{ML}, k_{600} and k_{H}) and their dependence on lake size (same as used earlier), the underestimation ratio becomes vanishingly small for large lakes (solid lines in Figure 5A), which would require unrealistically high bias correction. However, Monte Carlo simulations with realistic variabilities in the individual physical parameters (25% coefficient of variation for Z_{ML} and k_{600} and uniform distribution between k_{H1} and k_{H2}) for any given lake size also showed that this underestimation ratio becomes highly unstable as lake size increases. When we randomly added the impact of biological processes of magnitude and distribution equivalent to those found in our study lakes, the simulations combining the two sources of variability (physical and biological) displayed even more scatter for large lakes (gray dots, Figure 5A). For practical purposes, and in the absence of additional information on the exact physical parameters of a lake or the particular magnitude of the relevant biological processes, we used the simulated values (after binning the data) to generate a simple and general rule applicable to lakes between 100 and 5000 m in equivalent radius, *ER* (or ~ 0.03 and 80 km^2 in area), to approximate the likely underestimation bias as $1.56 - 0.37{*}\log_{10}(\mathrm{ER}\ [m])$ and $1.47 - 0.36{*}\log_{10}(\mathrm{ER}\ [m])$ for round and elongated lakes, respectively (Figure 5B). Unfortunately, the greater scatter in underestimation biases for large lakes not only prevents reasonable approximation of the bias in such lakes, but also illustrates their sensitivity to physical constraints and pelagic biological processes, of which little is known since they remain greatly under sampled. Regardless, the magnitude of the biases in small- and medium-sized lakes, which are the most often studied, is sufficiently large to warrant a reassessment of current approaches used to estimate CH_4 emissions from lakes.

The physical framework that we developed here rests on some key assumptions. The model assumes a single littoral source of CH_4 that is uniform throughout the lake perimeter. In reality, there may be local differences in littoral CH_4 production and release, for example, due to patchy macrophyte coverage or local heterogeneities in sediment composition or ebullition. Yet, the ability of our model to reproduce the spatial trends suggests that these differences are likely averaged out not only within a given lake but also across lakes. Gas transfer velocity is another key parameter but one that we feel is reasonably well constrained in our model since it varied with ecosystem size. Perhaps the least well-constrained parameter in our physical model is the horizontal diffusivity coefficient, k_{H}. There are surprisingly very few models of this key parameter, and those that exist differ in their respective predictions by several fold (Okubo 1971; Murthy 1976; Lawrence and others 1995; Peeters and Hofmann 2015), most likely because of the stochastic nature of horizontal mixing (Peeters and others 1996). However, the fact that we could effectively reconstruct the spatial pattern of radon, which is not influenced by biological processes and has a certain littoral origin, would suggest that our parameter bounds for k_{H} captured the magnitude of

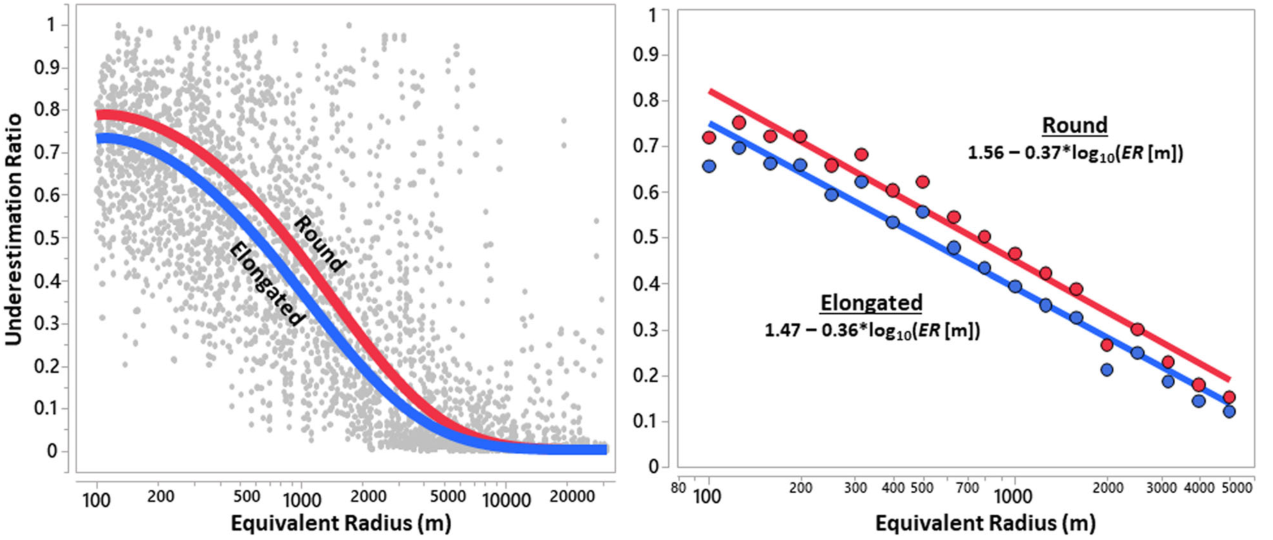

Figure 5. An underestimation bias, defined as the ratio of the center CH_4 concentration to a spatially integrated CH_4 concentration, can be induced if CH_4 is only sampled from the center of a lake and then used for upscaling system-wide CH_4 emissions. The underestimation for the round (*red line*) and elongated (*blue line*) models scales with lake size such that the center-to-integrated CH_4 ratio is closer to one in small lakes and the bias increases with lake size or equivalent radius, as shown here (derivation found in SI). **A** Lines show the bias induced by physics alone assuming constant k_{600}, Z_{ML} and k_H variables for each lake size, whereas the *gray dots* illustrate the result of random but realistic variability in both the physical and biological processes dictating surface CH_4 distribution. The variability was induced using Monte Carlo simulations (see text for details). **B** Following binning of the Monte Carlo simulations, a guideline for underestimation can be provided for lakes with an equivalent radius of 100–5000 m (or surface area from 0.03 to 80 km^2). Larger lakes are heavily influenced by variability in the processes dictating spatial CH_4 distribution, particularly the biological ones, and thus predicting resulting biases for lakes $>$ 100 km^2 is difficult (Color figure online).

lateral transport in our study lakes. Nevertheless, k_H certainly warrants further research as not only does it dictate the spatial behavior of CH_4, but also impacts other processes in lakes such as nutrient distribution, productivity and sediment resuspension, and ultimately links the major habitats present within lacustrine systems (Macintyre and Melack 1995). Finally, our integration of the biological oxidation/production processes within our modeling framework presented here represents only an initial attempt at constraining their relative roles in shaping the magnitude and spatial pattern of CH_4 concentration in stratified lakes. Lakes where surface waters are in direct contact with the sediments along the entire lake surface, such as shallow mixed lakes, should not follow the spatial patterns predicted by our physical model, and in addition, the relative importance of pelagic CH_4 production and oxidation would likely shift in this type of lake.

CONCLUSIONS

The physical model we developed to reconstruct littoral CH_4 transport and gas exchange effectively accounted for (1) the rather characteristic exponential decay in lake surface CH_4 that we observed with distance from shore, and (2) the negative relationship between lake size and both the average CH_4 and the magnitude of the exponential decline of CH_4 in each lake. However, the model tended to systematically under predict concentrations, particularly in the center of larger lakes. Although the overall under prediction by the model could be accounted for by variability in the physical parameterization of the model, the $\delta^{13}CH_4$ evidence suggests that biological processes indeed occurred and significantly influenced surface CH_4 distributions. The spatial distribution of both CH_4 concentration and $\delta^{13}CH_4$ appeared to reflect net biological removal of CH_4 in approximately 30% of the study lakes, based on the net enrichment trend of $\delta^{13}CH_4$ in those lakes. The spatial distribution in the remaining 70% of lakes that showed a consistent depletion in $\delta^{13}CH_4$, however, could not have been due to anything other than a net input from a CH_4 source with a more ^{13}C-depleted signal than that which was transported from the littoral zone. Although more work is needed to determine rates and mechanisms behind this epilimnetic CH_4 source in freshwaters, our results do indicate that CH_4 production is widespread across lake surface waters, and that this process along with horizontal transport of littoral CH_4 is likely the major cause of the ubiquitous CH_4 oversaturation observed in lakes globally. Finally, our empirical and model results strongly suggest that only sampling the center of lakes will induce an underestimation bias in CH_4 emission estimates of most lakes. We have provided an initial bias correction for upscaling system-wide emissions in a range of lake sizes, but more research is necessary to better constrain the true underestimation bias, particularly in large lakes where data on the relevant variables are scarce.

ACKNOWLEDGEMENTS

We would like to thank Martin Demers, Alexandre Ducharme, Karelle Desrosiers, Olivia del Giorgio, Alice Parkes, Annick St-Pierre and Katherine Velghe for field and laboratory assistance, as well as the staff at the Station de biologie des Laurentides (Université de Montréal), La Forêt d'Enseignement et de Recherche Simoncouche (Université du Québec à Chicoutimi) and L'Institut de recherché sur les forêts (Université du Québec en Abitibi-Temiscamingue). Also thank you to two anonymous reviewers for useful comments. This is a contribution to the Industrial Research Chair in Carbon Biogeochemistry in Boreal Aquatic Systems (CarBBAS), co-funded by the Natural Sciences and Engineering Research Council of Canada (NSERC) and Hydro-Québec, and to the UNESCO Chair in Global Environmental Change. The study was further supported by NSERC Discovery grants to Y. T. Prairie and P. A. del Giorgio and a Swiss National Science Foundation Advanced Postdoc Mobility grant awarded to T. DelSontro (P300P2_151253).

REFERENCES

Bastviken D, Cole J, Pace M, Tranvik L. 2004. Methane emissions from lakes: dependence of lake characteristics, two regional assessments, and a global estimate. Glob Biogeochem Cycles 18:GB4009.

Bastviken D, Ejlertsson J, Tranvik L. 2002. Measurement of methane oxidation in lakes: a comparison of methods. Environ Sci Technol 36:3354–61.

Bastviken D, Tranvik LJ, Downing JA, Crill PM, Enrich-prast A. 2011. Freshwater methane emissions offset the continental carbon sink. Science 331:50.

Bogard MJ, del Giorgio PA, Boutet L, Chaves MCG, Prairie YT, Merante A, Derry AM. 2014. Oxic water column methanogenesis as a major component of aquatic CH4 fluxes. Nat Commun 5:5350.

Crusius J, Wanninkhof R. 2003. Gas transfer velocities measured at low wind speed over a lake. Limnol Oceanogr 48:1010–17.

Damm E, Helmke E, Thoms S, Schauer U, Nöthig E, Bakker K, Kiene RP. 2010. Methane production in aerobic oligotrophic surface water in the central Arctic Ocean. Biogeosciences 7:1099–108.

DelSontro T, Boutet L, St-Pierre A, del Giorgio PA, Prairie YT. 2016. Methane ebullition and diffusion from northern ponds and lakes regulated by the interaction between temperature and system productivity. Limnol Oceanogr 61:S62–77.

DelSontro T, Mcginnis DF, Wehrli B, Ostrovsky I. 2015. Size does matter: importance of large bubbles and small-scale hot spots for methane transport. Environ Sci Technol 49:1268–76.

Fernández JE, Peeters F, Hofmann H. 2016. On the methane paradox: transport from shallow-water zones rather than in situ methanogenesis is the mayor source of CH_4 in the open surface water of lakes. J Geophys Res Biogeosci 121:2717–26.

Grossart H-P, Frindte K, Dziallas C, Eckert W, Tang KW. 2011. Microbial methane production in oxygenated water column of an oligotrophic lake. Proc Natl Acad Sci 108:19657–61.

Hanna M. 1990. Evaluation of models prediding mixing depth. Can J Fish Aquat Sci 47:940–7.

Happell JD, Chanton JP. 1994. The influence of methane oxidation on the stable isotopic composition of methane emitted from Florida swamp forests. Geochim Cosmochim Acta 58:4377–88.

Hofmann H. 2013. Spatiotemporal distribution patterns of dissolved methane in lakes: how accurate are the current estimations of the diffusive flux path? Geophys Res Lett 40:2779–84.

Hofmann H, Federwisch L, Peeters F. 2010. Wave-induced release of methane: littoral zones as source of methane in lakes. Limnol Oceanogr 55:1990–2000.

Juutinen S, Rantakari M, Kortelainen P, Huttunen JT, Larmola T, Alm J, Silvola J, Martikainen PJ. 2009. Methane dynamics in different boreal lake types. Biogeosciences 6:209–23.

Karl DM, Beversdorf L, Björkman KM, Church MJ, Martinez A, Delong EF. 2008. Aerobic production of methane in the sea. Nat Geosci 1:473–8.

Keeling C. 1958. The concentration and isotopic abundances of atmospheric carbon dioxide in rural areas. Geochim Cosmochim Acta 13:322–34.

Knox M, Quay PD, Wilbur DO. 1992. Kinetic isotopic fractionation during air-water gas transfer of O_2, N_2, CH_4, and H_2. J Geophys Res 97:20335–43.

Lawrence GA, Ashley KI, Yonemitsu N, Ellis JR. 1995. Natural dispersion in a small lake. Limnol Oceanogr 40:1519–26.

Macintyre S, Melack JM. 1995. Vertical and horizontal transport in lakes: linking littoral, benthic, and pelagic habitats. J N Am Benthol Soc 14:599–615.

McGinnis DF, Greinert J, Artemov Y, Beaubien SE, Wüest A. 2006. Fate of rising methane bubbles in stratified waters: how much methane reaches the atmosphere? J Geophys Res 111:C09007.

Murase J, Sakai Y, Kametani A, Sugimoto A. 2005. Dynamics of methane in mesotrophic Lake Biwa, Japan. Ecol Res 20:377–85.

Murase J, Sakai Y, Sugimoto A, Okubo K, Sakamoto M. 2003. Sources of dissolved methane in Lake Biwa. Limnology 4:91–9.

Murthy CR. 1976. Horizontal diffusion characteristics in Lake Ontario. J Phys Oceanogr 6:76–84.

Natchimuthu S, Sundgren I, Gålfalk M, Klemedtsson L, Crill P, Danielsson Å, Bastviken D. 2016. Spatio-temporal variability of lake CH_4 fluxes and its influence on annual whole lake emission estimates. Limnol Oceanogr 61:S13–26.

Okubo A. 1971. Oceanic diffusion diagrams. Deep Sea Res Oceanogr Abstr 18:789–802.

Ostrovsky I, McGinnis DF, Lapidus L, Eckert W. 2008. Quantifying gas ebullition with echosounder: the role of methane transport by bubbles in a medium-sized lake. Limnol Oceanogr Methods 6:105–18.

Peeters F, Hofmann H. 2015. Length-scale dependence of horizontal dispersion in the surface water of lakes. Limnol Oceanogr 60:1917–34.

Peeters F, Wuest A, Piepke G, Imboden DM. 1996. Horizontal mixing in lakes. J Geophys Res 101:18361–75.

Rasilo T, Prairie YT, del Giorgio PA. 2015. Large-scale patterns in summer diffusive CH_4 fluxes across boreal lakes, and contribution to diffusive C emissions. Glob Change Biol 21:1124–39.

Reeburgh W, Heggie D. 1977. Microbial methane consumption reactions and their effect on methane distributions in freshwater and marine environment. Limnol Oceanogr 22:1–9.

Rinta P, Bastviken D, Schilder J, Van Hardenbroek M, Stötter T, Heiri O. 2017. Higher late summer methane emission from central than northern European lakes. J Limnol 76:52–67.

Schilder J, Bastviken D, van Hardenbroek M, Kankaala P, Rinta P, Stötter T, Heiri O. 2013. Spatial heterogeneity and lake morphology affect diffusive greenhouse gas emission estimates of lakes. Geophys Res Lett 40:5752–6.

Schilder J, van Hardenbroek M, Bastviken D, Heiri O. 2016. Spatio-temporal patterns in methane flux and piston velocity at low wind speed: implications for upscaling studies on small lakes. J Geophys Res Biogeosci 121:1456–67.

Schmidt U, Conrad R. 1993. Hydrogen, carbon monoxide, and methane dynamics in Lake Constance. Limnol Oceanogr 38:1214–26.

Schubert CJ, Lucas FS, Durisch-Kaiser E, Stierli R, Diem T, Scheidegger O, Vazquez F, Müller B. 2010. Oxidation and emission of methane in a monomictic lake (Rotsee, Switzerland). Aquat Sci 72:455–66.

Stauffer RE. 1980. Windpower time series above a temperate lake. Limnol Oceanogr 25:513–28.

Tang KW, McGinnis DF, Ionescu D, Grossart H-P. 2016. Methane production in oxic lake waters potentially increases aquatic methane flux to air. Environ Sci Technol Lett 3:227–33.

Tang KW, McGinnis DG, Frindte K, Brüchert V, Grossart H-P. 2014. Paradox reconsidered: methane oversaturation in well-oxygenated lake waters. Limnol Oceanogr 59:275–84.

Vachon D, Prairie YT. 2013. The ecosystem size and shape dependence of gas transfer velocity versus wind speed relationships in lakes. Can J Fish Aquat Sci 70:1757–64.

Varadharajan C, Hemond HF. 2012. Time-series analysis of high-resolution ebullition fluxes from a stratified, freshwater lake. J Geophys Res Biogeosci 117:G02004.

Wang Q, Dore JE, Mcdermott TR. 2017. Methylphosphonate metabolism by pseudomonas sp. populations contributes to the methane oversaturation paradox in an oxic freshwater lake. Environ Microbiol 19:2366–78.

Whiticar MJ. 1999. Carbon and hydrogen isotope systematics of bacterial formation and oxidation of methane. Chem Geol 161:291–314.

Whiticar MJ, Faber E. 1986. Methane oxidation in sediment and water column environments—isotope evidence. Adv Org Geochem 10:759–68.

Wik M, Varner RK, Anthony KW, MacIntyre S, Bastviken D. 2016. Climate-sensitive northern lakes and ponds are critical components of methane release. Nat Geosci 9:99–106.

Yao M, Henny C, Maresca JA. 2016. Freshwater bacteria release methane as a by-product of phosphorus acquisition. Appl Environ Microbiol 82:6994–7003.